

## ULTRASONIC FATIGUE ANALYSIS ON STEEL SPECIMEN WITH TEMPERATURE CONTROL: EVALUATION OF VARIABLE TEMPERATURE EFFECT

Y. Lage, M. de Freitas, D. Montalvão, A.M.R. Ribeiro, L. Reis

Instituto Superior Técnico, ICEMS & IDMEC, Mechanical Engineering Department, Av. Rovisco Pais,  
1049-001 Lisboa, Portugal

### ABSTRACT

Ultrasonic fatigue testing machine are being used to perform materials testing in the range of  $10^9$  to  $10^{10}$  fatigue cycles. The so-called very high cycle fatigue regime is now under intense studies in which concerns the lay-out of ultrasonic fatigue testing machines. Nevertheless, the accurate measurement of the parameters that influence fatigue life (stress, strain, displacement ...) at ultrasonic frequencies still is a matter of concern and continuous development. The objective of this paper is to describe the design and construction of an ultrasonic fatigue testing machine at 20 kHz working frequency. In order to achieve fully automated tests, a closed loop control system was developed to use monitored temperature and displacement to set the power and the cooling periods of the machine. The monitoring of the displacement, considered here in the bottom face of the specimen, is carried out using a high resolution laser. The specimen's temperature is monitored online through a pyrometer. To manage and process, a data acquisition device working at 400 kHz from National Instruments is used. The software was developed in house using the LabView package. The present paper describes the advantages and drawbacks of metal fatigue testing at very high frequencies.

**KEYWORDS:** Very high cycle fatigue (VHCF); ultrasonic fatigue testing; temperature control; displacement control

### 1. INTRODUCTION

The necessity to increase performances in terms of lifetime and security in mechanical components or structures is the motivation for intense research. Have a proper knowledge of the damage and rupture mechanisms in materials fatigue at VHCF domain is extremely important nowadays. However, using conventional fatigue testing machine to carry out VHCF tests can be very time-consuming; for instance, making a fatigue test with hydraulic machine at 30 Hz as working frequency would take more than one year to reach  $10^9$  cycles.

The ultrasonic approach in fatigue testing procedures turns these tests practicable in a feasible way. It is possible achieve in few hours the fatigue strength at  $10^9$  cycles or even  $10^{10}$ , which is the utmost value of the range currently used in mechanical design. The advantages of the ultrasonic tests associated to the improvements in piezoelectric devices became the ultrasonic fatigue testing an attractive technique used around the world to establish SN curves in VHCF.

The piezoelectric techniques applied to fatigue tests started with Hopkinson in the beginning of the 20<sup>th</sup> century [1]. He created the first piezoelectric fatigue testing machine working in longitudinal resonance with 33 Hz. Fifty years later, in 1950, an ultrasonic fatigue testing machine with 20 kHz as working frequency was presented in scientific community by Mason. In the attempt to reach higher frequencies Girard presents in 1959 a testing machine with 92 kHz as testing frequency

but, at that time, some questions unanswered were made about the results; the technology available doesn't guarantee a convincing correlation between results and experiments.

The testing process creates some variables, which can affect the results in the lifetime fatigue [2]. The specimen temperature increase resulting from internal friction is one of them. To control that variable, the cooling of the specimen can be made with some refrigerants but that can result in variation of mechanical properties at the specimen surface [3]. Another solution is interrupting de test and wait for the specimen cools down but the transient regime due to the on/off cooling procedure may create additional internal damage in material lattice [4].

Nowadays, some issues were overcome but some scepticism still remains about some aspects, mainly the calculation of applied stresses and the temperature control of the specimens when tested at very high frequencies. Concerning the calculation of stresses, the development of new sensors and the analytical and computational calculations allow an accurate determination of applied stresses, the heating of the specimens continues unsolved. Two strategies are proposed: the continuous cooling of the specimen during the test [3], with temperatures approaching 100°C at steady state, or by using a pulse-pause sequence of the test [4], limiting the heating of the specimen but increasing the number of cycles at lower load in the transition phase. Therefore, the research in this field still is an actual subject.

The objective of this work is the design and instrumentation of an ultrasonic fatigue testing machine at 20 kHz working frequency; this machine must eliminate the unwanted effects of using high frequencies, such as temperature control and on-line stress analysis providing results compatible with the data obtained by lower frequencies. The method of investigation was implemented in the lab and workshop. Some components were acquired and adapted others machined. The fatigue testing requirements and the necessity of eliminating some issues unresolved in the instrumentation of these testing machines are the main reasons of the targets for this work.

## 2. FATIGUE TESTING MACHINE

The ultrasonic fatigue testing machine is an integrated system with several elements, each one of them with a specific task. The ultrasonic energy must be transmitted between resonant elements in an efficient way. This efficiency can be achieved due to the amplification granted by specific geometric properties of the elements at the longitudinal mode. That amplification lays down in one transmission line along the elements, starting in the actuator and ending at the specimen bottom. Along this line is provided a change in the amplitude of vibration, which means different levels of axial stress along all elements [1, 5]. In Fig. 1 is represented the booster, horn and specimen with the typical evolution of displacement and stress along the amplification line.

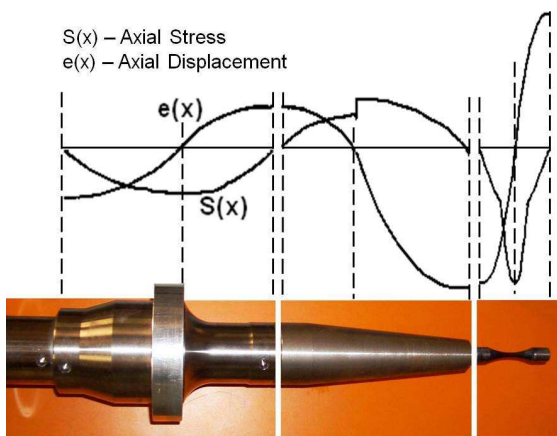


Figure 1. Amplification line along the elements

Fig. 2 shows the system implemented at IST laboratory. All resonant elements are mechanically connected by a screw connection; the piezoelectric actuator is connected to the booster who in turn is connected to the horn. The specimen is connected to the end of the horn. These four elements form the resonant system of the testing machine. The actuator is headed through the signal generator who in turn is controlled through one control box, this box is commanded through one LabView routine. The lasers and pyrometer are connected to the data acquisition device, DAQ.

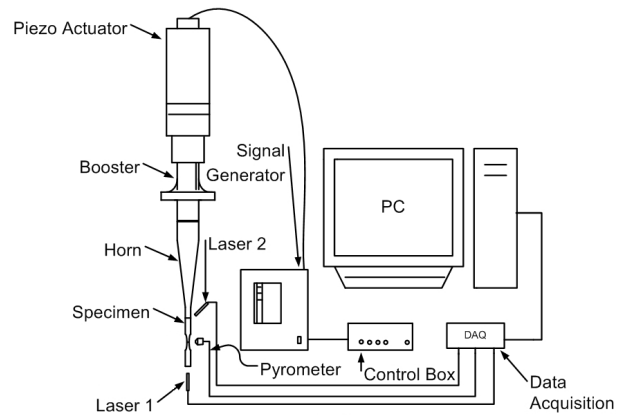


Figure 2. System and connection layout

### 2.1. Machine Elements

The piezoelectric actuator converts electrical signals into mechanical vibrations and needs to be headed by one signal generator. The piezoelectric actuator used is a 2.2 kW Branson transducer with 20 kHz as working frequency and 20  $\mu\text{m}$  peak to peak of maximum displacement. The generator delivers to the transducer an electric signal with a sinusoidal shape and predetermined resonant frequency. The signal generator selected, is a Branson DC222 with [19.5 – 20.5] KHz as working frequency range. The resonant frequency is determined by the signal generator through a frequency scan.

The objectives of using one horn, is amplifying the displacements delivered by the booster and allow the connectivity between the specimen test and the resonant system. The horn and the specimen test was designed with a finite element routine and machined in the workshop.

The specimen test (displacement, strain, stress) is monitored with one laser transducer which measures the displacement and the phase angle in the specimen along the fatigue test. The laser used has a laser autofocus measurement principle with a 0.260 mm as measurement range and resolution down to 5 nm at frequency responses up to 200 kHz.

A pyrometer is used to monitor on-line the temperature of the specimen; the objective is monitoring de temperature and sends that information to the lab view routine through the DAQ device. This pyrometer have a [- 40°C to 600°C] as measure range, the accuracy is about 1% or  $\pm 1^\circ\text{C}$  and have a 150 ms as response time.

The information delivered by the monitoring elements is processed by a data acquisition device which is the interface between the peripherals and the LabView routine.

The NI USB-6216, is a bus-powered USB M Series multifunction data acquisition (DAQ) device optimized for fast sampling rates: 16 analogue inputs, 400 kS/s

sampling rate, two analogue outputs, 32 digital I/O lines, four programmable input ranges ( $\pm 0.2$  to  $\pm 10$  V) per channel, digital triggering and two counter/timers.

2.2. Monitoring

The machine calibration is implemented with the relation between the power applied and the displacement at specimen test extremities. Due to the several amplification levels in the resonant system the lasers are a useful tool which permits to achieve accurate results in the axial stress prediction and monitoring the specimen mechanical behaviour during the fatigue test, as example, the hysteretic damping can be analysed with these two lasers and dynamic elastic modulus can be determined. The fatigue test monitoring is performed with a LabView routine, Fig. 3, which receive signals from the monitoring system through the DAQ device. This routine determines the testing frequency, establishes the power delivered to the piezoelectric actuator to achieve the desired axial tension, indicate the specimen temperature history and the number of cycles at rupture time. When the fatigue test is finished a summary with the monitoring history is shown.

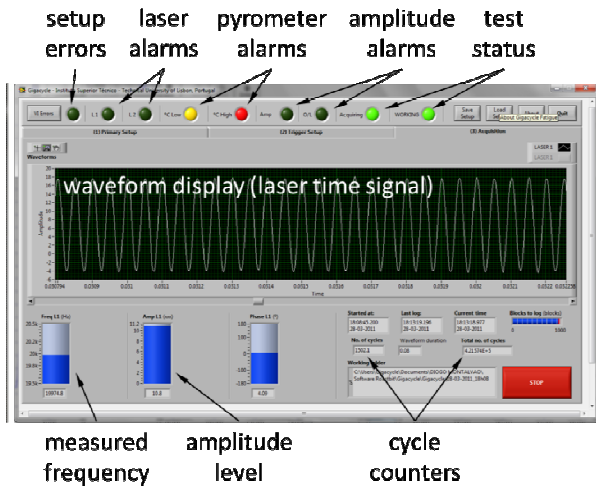


Figure 3. Control panel of LabView routine

2.3. Analytical specimen design

Under longitudinal resonance [1, 5], the specimen behaviour must satisfy the differential Eq. (1), determined by the equilibrium of forces.

$$\frac{\partial^2 u(x,t)}{\partial x^2} + P(x) \frac{\partial u(x,t)}{\partial x} = \frac{1}{C^2} \frac{\partial^2 u(x,t)}{\partial t^2} \quad (1)$$

Considering the following variable change, applied to Eq. (1):

$$u(x,t) = U(x) \sin(\omega t) \quad (2)$$

the amplitude of vibration  $U(x)$  at each point along the specimen can be easily obtained by:

$$U''(x) + P(x)U'(x) = -\frac{\omega^2}{C^2}U(x) \quad (3)$$

Considering the appropriated boundary conditions in the specimen, see Fig. 4, the differential solution divided in two parts is achieved, see Eq. (4) and Eq. (5).

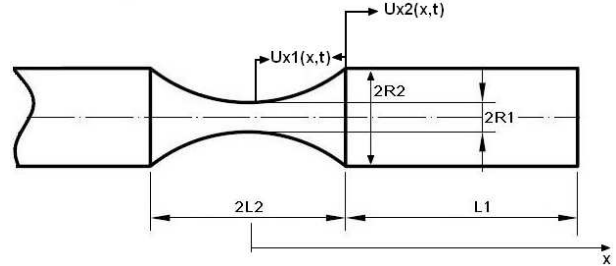


Figure 4. Standard specimen test geometry.

$$U_1(x) = \frac{C_1 \exp(\beta x) + C_2 \exp(-\beta x)}{\cosh(\alpha x)}, x < L_2 \quad (4)$$

$$U_2(x) = C_3 \cos(kx) + C_4 \sin(kx), L_2 < x \leq L \quad (5)$$

The constants  $C_1, C_2, C_3$  and  $C_4$  are determined with the resonant boundary conditions. Eq. (6) and Eq. (7) represent the displacement behaviour at longitudinal mode.

$$u_1(x,t) = \frac{A_0 \cos(kL_1) \cosh(\alpha L_2)}{\sinh(\beta L_2)} \frac{\sinh(\beta x)}{\cosh(\alpha x)} \sin(\omega t), x < L_2 \quad (6)$$

$$u_2(x,t) = A_0 \cos(k(L-x)) \sin(\omega t), L_2 < x \leq L \quad (7)$$

where  $A_0$  is the displacement amplitude at the end of the specimen. These two solutions represent the longitudinal resonance regime of the specimen in two different regions. In the interface between these regions the displacement must be the same.

$$u_1(x=L_2,t) = u_2(x=L_2,t) \quad (8)$$

Therefore selecting a value for the hyperbolic length,  $L_2$ , the expression for the cylindrical length is achieved. It is reached easily the characteristic dimension of the specimen test with the Eqs. (9) to (13).

$$L_1 = \frac{1}{k} \operatorname{arctg} \left[ \frac{\beta \coth(\beta L_2) - \alpha \tanh(\alpha L_2)}{k} \right] \quad (9)$$

$$\alpha = \frac{1}{L_2} \operatorname{arccos} h \left( \frac{R_2}{R_1} \right) \quad (10)$$

$$k = \sqrt{\frac{\omega^2}{C^2}} \quad (11)$$

$$\beta = \sqrt{\alpha^2 - k^2} \quad (12)$$

$$C = \sqrt{\frac{E_d}{\rho}} \quad (13)$$

where  $\omega$  is the resonance frequency in rad/s.

In Fig. 5 is represented one specimen test dimensions made with 42CrMo4, where the dimensions were calculated following the previous formulation.

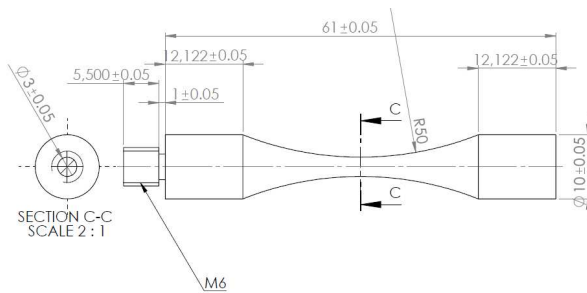


Figure 5. Specimen dimensions for ultrasonic fatigue (mm)

#### 24. Working procedures

To initiate the testing process, it is necessary to follow some procedures. The signal generator must be started and the last working frequency reset. It is necessary to perform the seek frequency procedure to allocate in the signal generator the new system resonant frequency. At this point the fatigue test may be started with the signal send by the LabView routine. A detailed description of the procedure is described in [6].

During the fatigue test, the signals from the ultrasonic transducers, the lasers and pyrometer are acquired and stored in order to monitor the specimen behaviour. When the bottom laser sends no information about the displacement signal the test is stopped. At this point the number of cycles at rupture and the specimen temperature history are registered.

### 3. RESULTS AND DISCUSSION

The machine has been fully implemented and successful fatigue tests in VHCF regime were carried out within temperature control where the temperature variation  $\Delta T$  and amplitude displacement are set before the test starts.

A test was conducted with a 42CrMo4 steel specimen as shown in Fig. 4, presenting a natural frequency close to 20 kHz ( $\approx 19.9$  kHz). The actuator power was set to 35% (770 W) and the operating temperature range  $\Delta T$ , from 28 °C to 40 °C. With a 200 kHz sampling frequency, each acquisition block lasted 0.1 s. Hence, the feedback loop was updated every 1000 cycles.

Due to the temperature control on the throat of the specimen during the fatigue test, the test is stopped every time the temperature reaches the maximum, followed by the cooling period till the minimum

temperature on the specimen throat is reached. Fig. 6 shows the detail of some running periods of heating (a) and cooling (b) times, between 28°C and 40°C ( $\Delta T$ ). A shorter or longer temperature range may be assigned, depending of the material and fatigue test conditions, therefore the duration of the test will depend strongly on the temperature range ( $\Delta T$ ) required due the cooling periods.

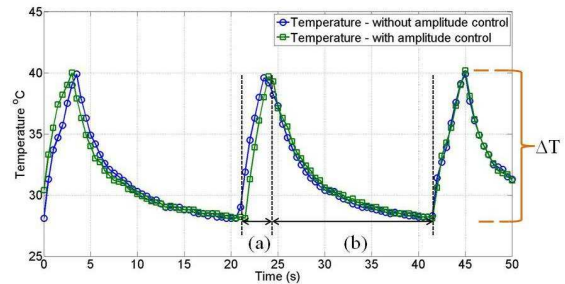


Figure 6. Evolution of the temperature during the fatigue test, showing heating (a) and cooling (b) time

Concerning the displacement amplitude measurement and control, two possibilities can be achieved on the test: a) with power fixed, i. e. setting the power on the piezoelectric actuator and having no control on the amplitude of the displacement; b) with amplitude displacement control, i. e. setting a fixed displacement at the bottom of the specimen which is related to the strain and stress at the centre of the specimen and therefore with the variation of the power.

The following results show the data acquisition of the resonant frequency of the test, the temperature evolution at the centre of the specimen and the displacement at the bottom of the specimen. These results show the effect of temperature increase on frequency and displacement amplitude with the testing at high frequencies.

Fig. 7 shows the evolution of the testing frequency during a fatigue test of  $2 \times 10^8$  cycles for both test conditions with or without amplitude control. It can be seen that after a relatively very short period of time, but a large number of cycles, the frequency stabilises at a slightly lower frequency than the required one and no significant differences are obtained with or without amplitude control.

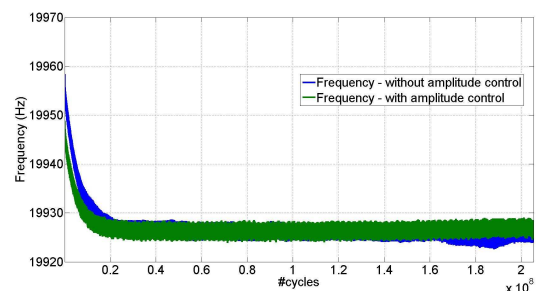


Figure 7. Evolution of the testing frequency

Fig. 8 shows a short detail of the data of Fig. 7 measured on steady state showing 5 collection of data acquisition (frequency). It clearly shows a decrease of the frequency with the heating of the specimen, but no significant effect in frequency is achieved, only 3 Hz from 19925 Hz to 19928 Hz.

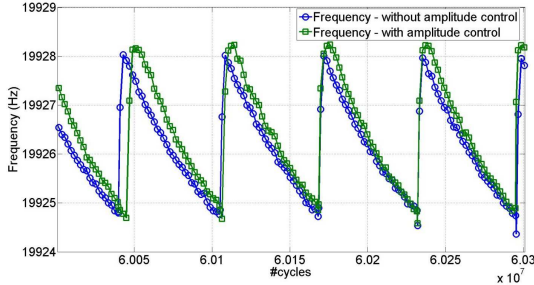


Figure 8. Detail of the testing frequency for a very short period of time.

The effect of displacement amplitude control on the power transmitted to the specimen is shown in Fig. 9. Without displacement amplitude control, the power transmitted to piezoelectric actuator remains fixed, 35% for the present results. The control of the displacement amplitude made at every block of cycles (0.1 s) implies a variation on the power transmitted to the piezoelectric actuator which is carried out by the developed software, therefore a closed loop fatigue testing machine is achieved.

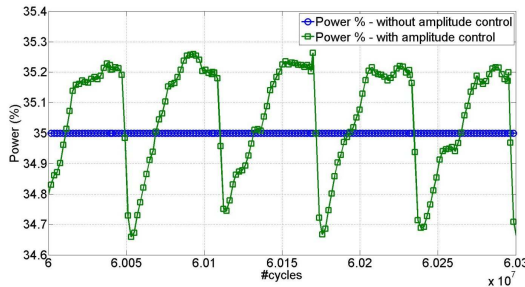


Figure 9. Evolution of the power during fatigue test

As mentioned in previous sections, the amplitude of the displacement is measured at the bottom of the specimen by the laser transducer. Fig. 10 shows the results of the measured displacement amplitudes during the  $2 \times 10^8$  cycles on the fatigue test, with and without amplitude control. The results of the measured amplitudes during the test follow a similar trend of the frequency shown in Fig. 6, i. e. after a very short period of time, a steady state of amplitude displacement is achieved and remains constant during the fatigue test. But, as can be seen in Fig. 9, the difference between the initial amplitude displacement at the beginning of the test is significant different from the amplitude displacement in steady state. Therefore, when programming a fatigue test. The effect of temperature must be taken into account. The advantage of amplitude control is that the steady state is achieved in a much faster way.

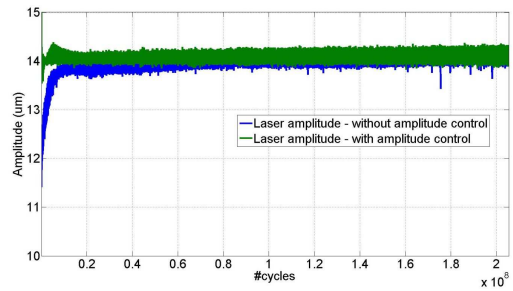


Figure 10. Displacement amplitude during fatigue test

A much more detailed observation of the results is shown in Fig. 11. A different behaviour is observed on the magnitude of the amplitude of the displacement with or without amplitude control. Without displacement amplitude control, the effect of temperature variation within the specified  $\Delta T$ , is to reduce the displacement amplitude on the specimen. In the condition of displacement amplitude control, a much more stable data is obtained and, with the exception of the first set of data, the displacement amplitude remains constant during the testing (heating) period.

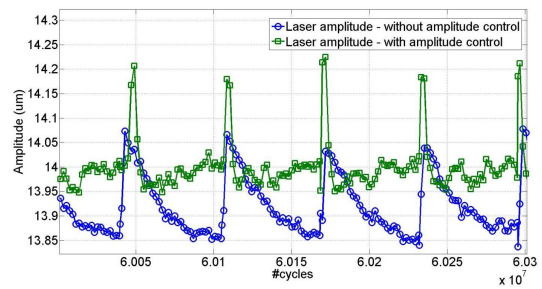


Figure 11. Detail of the displacement amplitude during fatigue test

The strain and stress amplitudes applied to the specimen can be easily determined from analytical expressions or by Finite Element Modelling. Using the same formulation presented in previous section for the calculation of the displacements, Eq. (6) and Eq. (7) and by differentiation of these equations, we obtain

$$\varepsilon_i = \frac{\partial U_i(x)}{\partial x} \quad (14)$$

For the hyperbolic part (1) of the specimen in Fig. 4:

$$\varepsilon_1(x) = A_0 \frac{\cos(kL_1) \cosh(\alpha L_2)}{\sinh(\beta L_2)} \left[ \frac{\beta \cosh(\beta x) \cosh(\alpha x) - \alpha \sinh(\beta x) \sinh(\alpha x)}{\cosh^2(\alpha x)} \right] \quad (15)$$

and for the cylindrical part (2) of the specimen in Fig. 4

$$\varepsilon_2(x) = A_0 k \sin(k(L-x)) \quad (16)$$

The stress distribution on the specimen can be easily calculated through the knowledge of the dynamic elastic modulus,  $E_d$ :

$$\sigma_i(x) = E_d \varepsilon_i(x) \quad (17)$$

and finally the following equations are obtained for the stresses at any point of the specimen:

$$\sigma_1(x) = E_d A_0 \frac{\cos(kL_1) \cosh(\alpha L_2)}{\sinh(\beta L_2)} \left[ \frac{\beta \cosh(\beta x) \cosh(\alpha x) - \alpha \sinh(\beta x) \sinh(\alpha x)}{\cosh^2(\alpha x)} \right] \quad (18)$$

$$\sigma_2(x) = E_d A_0 k \sin(k(L-x)) \quad (19)$$

respectively for the hyperbolic part (1) and for the cylindrical part (2) of the specimen.

Fig. 12 shows the stress amplitude on the throat of the specimen, calculated from Eq. (19). It shows clearly that with the amplitude control, the stress amplitude during the fatigue test is within the stress variation which is obtained in classical fatigue testing machines.

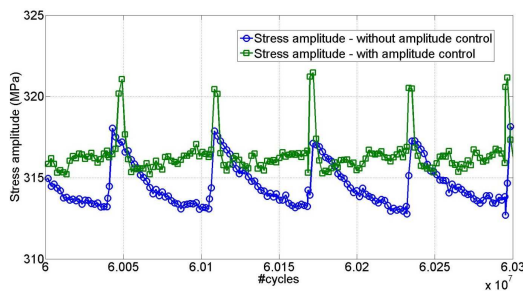


Figure 12. Stress amplitude on the throat of the specimen

The ultrasonic fatigue testing machine seems to be a good solution to the VHCF tests. The piezoelectric actuators are an easy way to reach high frequencies at high power levels. The fatigue results are obtained in a shorter time with lower costs compared to traditional fatigue test machines, which uses in most cases hydraulic mechanisms with much lower working frequencies and much more expensive.

#### 4. CONCLUSIONS

An ultrasonic fatigue testing machine was designed and assembled, verifying the resonant condition in the system with expected operating results.

Optimized geometries for the horn and specimen were designed and produced with resonance frequency under the piezoelectric actuator working frequency range.

The instrumentation of the specimen allowed the monitoring of the temperature of the specimen and the

displacement amplitude of the bottom of the specimen in a closed loop control.

Fatigue tests in VHCF regime were conducted with success, with any controlled temperature at specimen throat and controlled displacement amplitude at the bottom of the specimen.

The effect of heating on the specimen throat was monitored. The effect of heating on frequency, for low temperature ranges testing is negligible, but a significant effect on the displacement amplitude due to the heating of the specimen was observed and when programming fatigue tests this condition must be taken into account.

#### ACKNOWLEDGEMENTS

The authors gratefully acknowledge financial support from FCT - Fundação para Ciência e Tecnologia through the project PTDC/EME-PME/69904/2006.

#### REFERENCES

- [1] Bathias C, Paris PC. Gigacycle fatigue in mechanical practice. New York: Marcel Dekker; (2005).
- [2] Stanzl-Tschegg S. Very High Cycle Fatigue measuring techniques. Proceedings of the 5<sup>th</sup> International Conference on Very High Cycle Fatigue, Berlin, Germany, 2011, 3 – 17.
- [3] Bathias C. Piezoelectric fatigue testing machines and devices. International Journal of Fatigue (2006) 28, 1438 – 1445.
- [4] Mayer H. Ultrasonic torsion and tension-compression fatigue testing: Measuring principles and investigations on 2024-T351 aluminium alloy. International Journal of Fatigue (2006) 28, 1446 – 1445.
- [5] Freitas M, Reis L, Anes V, Montalvão D, Ribeiro AM and Fonte M. Design and assembly of an ultrasonic fatigue testing machine. Anales de Mecânica de la Fractura, 29, Vol. 1, 335 – 340.
- [6] Anes V, Montalvão D, Ribeiro AM, Freitas M and Fonte M. Design and instrumentation of an ultrasonic fatigue testing machine. Proceedings of the 5<sup>th</sup> International Conference on Very High Cycle Fatigue, Berlin, Germany, 2011, 421 – 426.